Passive-guaranteed modeling and simulation of a finite element nonlinear string model

David Roze, Mathis Raibaud, Thibault Geoffroy

Passive-guaranteed modeling and simulation of a finite element nonlinear string model

David Roze * **Mathis Raibaud** * **Thibault Geoffroy** *,**

* *Sciences et Technologies de la Musique et du Son, IRCAM - CNRS - SU UMR 9912, 1 place Igor Stravinsky, 75004 Paris, France (e-mail: david.roze@ircam.fr).*
** *Squarp SAS, 12 rue Marceau, 93100 Montreuil, France*

Abstract: This paper proposes to solve the dynamics of the Kirchhoff-Carrier nonlinear string model using the finite elements method. In order to ensure the power balance of the resulting finite dimensional model it is rewritten in the Port-Hamiltonian System (PHS) formalism. Using a discrete gradient and a quadratization of the Hamiltonian, an explicit power-preserving numerical scheme is proposed. Results of simulation are presented.

Keywords: Distributed parameter systems, Numerical Methods, Hamiltonian dynamics, Port-Hamiltonian systems, Quadratization, Nonlinear string model, Finite elements method

1. INTRODUCTION

Sound synthesis based on physical modeling relies on the resolution of dynamical problems to produce sound. In order to improve the realism of simulations, nonlinear phenomena should be included in physical models in order to describe properly the dynamics of musical instruments.

These nonlinear phenomena can be classified into two categories: (i) Interactions, that describe the transfer of energy between the musician and the instrument (e.g. bowing a string, striking a cymbal, the effect of lips or reeds in wind instruments, etc.), or between different resonating parts of the instrument (e.g. the transfer of energy between a string and a plate through a bridge, etc.). (ii) Geometric nonlinear terms that can be caused by large strains or displacements in one or several resonators.

The aim of this paper is to propose a framework to compute nonlinear dynamics in the latter case, i.e. for geometric nonlinearities. In the context of sound synthesis, stable and robust computations are expected in order to ensure a result (in real time if possible), even for geometries and physical parameters which may have very different values that the ones met in reality. In order to do this, the Port-Hamiltonian formalism (see Maschke et al. (1992); van der Schaft and Maschke (2002)) will be used. This formalism encodes the power balance of the system, this ensures all the energy transfers (between energy-storing components, with the outside of the system at the boundaries, or due to damping) are correctly modeled. The main advantage of this approach is that using numerical schemes that preserve this power balance (based for example on a discrete gradient (see Itoh and Abe (1988))) in the discrete time domain, stability and robustness of simulations should be guaranteed, even in the case of nonlinear dynamics (see Lopes et al. (2015)).

In the context of virtual instrument making the Finite Elements Method (FEM) is often used for the spatial discretization. This paper will address the most simple example of nonlinear resonator, namely the Kirchhoff-Carrier string model (see Kirchhoff (1877); Carrier (1945)) in order to present the formalism. This model has been extensively studied (see Narasimha (1968), Anand (1969)) and lead to three dimensional nonlinear models in e.g. Watzky (1992); Valette and Cuesta (1993). Several approaches have been proposed to get simulation results such as: finite differences with energy conservation in Bilbao (2009), or a FEM approach preserving a discrete energy in Chabassier and Joly (2010); Chabassier (2012).

On the other hand, the spatial discretization of Port-Hamiltonian systems has been a major research topic for the past two decades as it can be seen in Rashad et al. (2020). Regarding the discretization based on finite elements, a first approach has been presented in Golo et al. (2004) using Mixed Elements Methods (see Boffi et al. (2013)). More recently, a weak form of the Stokes-Dirac structure has been introduced in exterior calculus in order to be discretized (see Kotyczka et al. (2018)). In Cardoso-Ribeiro et al. (2020) Partitioned Finite Elements Method (PFEM) is presented and relies on a discretization of the weak form of the infinite dimensional system, then the integration by parts is done only on one of the two conservation laws, leading to a specific choice of boundary variables. Most of the works presented and mentioned in those references are about linear systems, but several recent results (such as Brugnoli and Matignon (2022) and Thoma and Kotyczka (2022)) have been published for nonlinear ones. All these works are based on the requirement to preserve the Port-Hamiltonian structure and properties (interconnection in the Stokes-Dirac structure

⋆ The training period of Thibault Geoffroy during which part of this research was made, was funded by Squarp SAS.

and constitutive laws based on the Hamiltonian) in the finite dimensional model.

The present work relies on the finite elements formulation of the nonlinear string model which is rewritten as a finite dimensional Port-Hamiltonian System. Usually an implicit numerical scheme based on an iterative solver is required. However, in this paper an explicit numerical scheme based on the discrete gradient will be proposed by applying a quadratization procedure (see Lopes et al. (2015)) to this non quadratic Hamiltonian.

This paper will present research done in Raibaud (2018); Geoffroy (2019) where the finite elements formulation of the Kirchhoff-Carrier string model is rewritten as a finite dimensional Port-Hamiltonian system (section 2). Boundary conditions will be applied using Lagrange multipliers as proposed in van der Schaft (2013). Finally, numerical scheme is introduced in section 3, and results of simulation are presented and commented in section 4.

2. A PASSIVE-GUARANTEED FINITE ELEMENTS STRING MODEL

2.1 The Kirchhoff-Carrier string model

The Kirchhoff-Carrier string model (see Carrier (1945)) is a nonlinear partial differential equation describing the transverse displacement in a plane $w : \Omega \times \mathbb{R}^+ \to \mathbb{R}$ (with $\Omega = [0, L]$) of a string of length L:

$$\mu\partial_{tt}w(\xi,t) + \alpha\partial_t w(\xi,t) = \left(T_0 + \frac{EA}{2L}\int_0^L \left(\partial_\xi w(\xi,t)\right)^2 \mathrm{d}\xi\right)\partial_{\xi\xi}w(\xi,t) + f(\xi,t), \quad (1)$$

where μ is the linear density, α the fluid damping, T_0 the tension at rest, E the Young's modulus and A the cross-sectional area. Longitudinal waves and polarization in the transverse plane of the string are neglected.

The nonlinear term is an approximation of the variation of tension due to the large deformations and will be rewritten as

$$T_0\left(1 + \epsilon\int_0^L \left(\partial_\xi w(\xi,t)\right)^2 \mathrm{d}\xi\right)\partial_{\xi\xi}w(\xi,t) = \mathcal{T}(t)\partial_{\xi\xi}w(\xi,t),$$

with $\epsilon = \frac{EA}{2LT_0}$.

Consider a state (see Wijnand et al. (2022)): $x = \begin{bmatrix} q(\xi,t) = \partial_\xi w(\xi,t) \\ p(\xi,t) = \mu\partial_t w(\xi,t) \end{bmatrix}$, the pH formulation writes

$$\begin{bmatrix} \partial_t q(\xi,t) \\ \partial_t p(\xi,t) \end{bmatrix} = \left(\begin{bmatrix} 0 & \partial_\xi \\ \partial_\xi & 0 \end{bmatrix} - \begin{bmatrix} 0 & 0 \\ 0 & \alpha \end{bmatrix}\right)\delta_x\mathcal{H}(x) + \begin{bmatrix} 0 \\ 1 \end{bmatrix} f(\xi,t)$$
$$y = \begin{bmatrix} 0 & 1 \end{bmatrix}\delta_x\mathcal{H}(x)$$

with the Hamiltonian

$$H(x) = \frac{1}{2}\int_0^L \left(\frac{(p^2(\xi,t))}{\mu} + T_0\left(1 + \frac{\epsilon}{2}\int_0^L q^2(\zeta,t)\mathrm{d}\zeta\right)q^2(\xi,t)\right)\mathrm{d}\xi,$$

and the variational derivative $\delta_x\mathcal{H}(x) = \begin{bmatrix} \mathcal{T}(t)q(\xi,t) \\ \dfrac{p(\xi,t)}{\mu} \end{bmatrix}$.

2.2 Weak formulation

Choosing the Dirichlet boundary conditions $w(0,t) = w(L,t) = 0, \forall t \in \mathbb{R}^+$, the weak formulation is obtained by multiplying (1) by a test function $v^*(\xi) \in H_0^1(\Omega)$, where $H_0^1(\Omega)$ is the Sobolev space $H_0^1(\Omega) = \{v \text{ s.t. } v \in H^1(\Omega), v|_{\partial\Omega} = 0\}$. After integration by parts and using the boundary conditions this yields

$$\int_0^L \mu\partial_{tt}wv^*\mathrm{d}\xi + \int_0^L \alpha\partial_t wv^*\mathrm{d}\xi = -\int_0^L \mathcal{T}(t)\partial_\xi w\partial_\xi v^*\mathrm{d}\xi + \int_0^L fv^*\mathrm{d}\xi. \quad (2)$$

2.3 Discretization and interpolation

In this paper space discretization relies on $\mathbb{P}_1$ (linear) Lagrange elements of length $h = \frac{L}{n}$ using Galerkin method. In one element, displacement at each point $\xi \in [0, h]$ will be approximated by

$$w(\xi,t) \approx w_1(t)\phi_1(\xi) + w_2\phi_2(\xi),$$

where w_1 and w_2 are the respective displacements of the two neighbour nodes and ϕ_i are the basis functions of interpolation. Choosing linear basis functions $\phi_1(\xi) = \frac{h-\xi}{h}$ and $\phi_2(\xi) = \frac{\xi}{h}$, displacement can be written as

$$w(\xi,t) \approx \begin{bmatrix} \phi_1(\xi) & \phi_2(\xi) \end{bmatrix}\begin{bmatrix} w_1(t) \\ w_2(t) \end{bmatrix} = \boldsymbol{\Phi}^T(\xi)\boldsymbol{W}_e(t).$$

Similarly, defining $v^*(\xi) \approx \boldsymbol{\Phi}^T(\xi)\boldsymbol{V}_e$ and $f(\xi,t) \approx \boldsymbol{\Phi}^T(\xi)\boldsymbol{F}_e(t)$, weak formulation (2) can be rewritten on a single element

$$\int_0^h \mu\boldsymbol{V}_e^T\underbrace{\boldsymbol{\Phi}\boldsymbol{\Phi}^T}_{\boldsymbol{M}_e}\partial_{tt}\boldsymbol{W}_e\mathrm{d}\xi + \int_0^h \alpha\boldsymbol{V}_e^T\underbrace{\boldsymbol{\Phi}\boldsymbol{\Phi}^T}_{\boldsymbol{M}_e}\partial_t\boldsymbol{W}_e\mathrm{d}\xi = -\int_0^h T(t)\boldsymbol{V}_e^T\underbrace{\partial_\xi\boldsymbol{\Phi}\partial_\xi\boldsymbol{\Phi}^T}_{\boldsymbol{K}_e}\boldsymbol{W}_e\mathrm{d}\xi + \int_0^h \boldsymbol{V}_e^T\underbrace{\boldsymbol{\Phi}\boldsymbol{\Phi}^T}_{\boldsymbol{M}_e}\boldsymbol{F}_e\mathrm{d}\xi,$$

with the global nonlinear coefficient

$$T(t) = T_0\left(1 + \epsilon\int_0^L \boldsymbol{W}^T\underbrace{\partial_\xi\boldsymbol{\Phi}\partial_\xi\boldsymbol{\Phi}^T}_{\boldsymbol{K}}\boldsymbol{W}\mathrm{d}\xi\right)$$

where $\boldsymbol{W}$ and $\boldsymbol{K}$ are defined by the assembly step (cf. section 2.4).

Factorizing by $\boldsymbol{V}_e^T$, equilibrium equation for one element writes

$$\mu\boldsymbol{M}_e\partial_{tt}\boldsymbol{W}_e + \alpha\boldsymbol{M}_e\partial_t\boldsymbol{W}_e + T(t)\boldsymbol{K}_e\boldsymbol{W}_e = \boldsymbol{M}_e\boldsymbol{F}_e,$$

with the elementary, mass matrix $\mu\boldsymbol{M}_e$, damping matrix $\alpha\boldsymbol{M}_e$, and stiffness matrix $\boldsymbol{K}_e$.

2.4 Assembly: The Port-Hamiltonian System

Global matrices for the whole system are defined by assembly, i.e. elementary matrices are concatenated and components associated to a same node are summed,

$$\tilde{\boldsymbol{M}} = \frac{1}{6}\begin{bmatrix} 2h & h & \cdots & 0 & 0 \\ h & 4h & \cdots & 0 & 0 \\ \vdots & \vdots & \vdots & \vdots & \vdots \\ 0 & 0 & \cdots & 4h & h \\ 0 & 0 & \cdots & h & 2h \end{bmatrix}, \tilde{\boldsymbol{K}} = \frac{1}{h}\begin{bmatrix} 1 & -1 & \cdots & 0 & 0 \\ -1 & 2 & \cdots & 0 & 0 \\ \vdots & \vdots & \vdots & \vdots & \vdots \\ 0 & 0 & \cdots & 2 & -1 \\ 0 & 0 & \cdots & -1 & 1 \end{bmatrix}.$$

Defining $\boldsymbol{M} = \mu\tilde{\boldsymbol{M}}$, $\mathbf{C} = \alpha\tilde{\boldsymbol{M}}$, $\boldsymbol{K} = \tilde{\boldsymbol{K}}$ and $\boldsymbol{F} = \tilde{\boldsymbol{M}}\tilde{\boldsymbol{F}}$ (where $\tilde{\boldsymbol{F}}$ is the vector of concatenated elementary forces $\boldsymbol{F}_e$) the finite elements formulation can be written

$$\boldsymbol{M}\partial_{tt}\boldsymbol{W} + \mathbf{C}\partial_t\boldsymbol{W} + T_0\left(1 + \epsilon\boldsymbol{W}^T\boldsymbol{K}\boldsymbol{W}\right)\boldsymbol{K}\boldsymbol{W} = \boldsymbol{F}.$$

This equilibrium equation can be rewritten in the Port-Hamiltonian Systems framework (see Maschke et al. (1992)).

The state vector $\boldsymbol{X} = \begin{pmatrix}\boldsymbol{W}\\ \boldsymbol{P}\end{pmatrix}$ is made of the nodes positions $\boldsymbol{W}$ and momenta $\boldsymbol{P} = \boldsymbol{M}\partial_t\boldsymbol{W}$. The discretized version of the Hamiltonian writes

$$H(\boldsymbol{X}) = \frac{1}{2}\left(\boldsymbol{P}^T\boldsymbol{M}^{-1}\boldsymbol{P} + T_0\left(1 + \frac{\epsilon}{2}\boldsymbol{W}^T\boldsymbol{K}\boldsymbol{W}\right)\boldsymbol{W}^T\boldsymbol{K}\boldsymbol{W}\right) \tag{3}$$

leading to the following PHS

$$\begin{pmatrix}\partial_t\boldsymbol{W}(t)\\ \partial_t\boldsymbol{P}(t)\end{pmatrix} = \begin{pmatrix}\mathbf{0}_N & \boldsymbol{I}_N\\ -\boldsymbol{I}_N & -\mathbf{C}\end{pmatrix}\begin{pmatrix}T(t)\boldsymbol{K}\boldsymbol{W}(t)\\ \boldsymbol{M}^{-1}\boldsymbol{P}(t)\end{pmatrix} - \begin{pmatrix}\mathbf{0}_N\\ -\boldsymbol{I}_N\end{pmatrix}\boldsymbol{F}(t), \tag{4}$$

$$\boldsymbol{M}^{-1}\boldsymbol{P}(t) = \begin{pmatrix}\mathbf{0}_N & \boldsymbol{I}_N\end{pmatrix}\begin{pmatrix}T(t)\boldsymbol{K}\boldsymbol{W}(t)\\ \boldsymbol{M}^{-1}\boldsymbol{P}(t)\end{pmatrix}. \tag{5}$$

2.5 Boundary conditions: algebraic constraints

Homogeneous Dirichlet boundary conditions can be defined by removing the associated degrees of freedom. However, in this work boundary conditions will be defined as algebraic constrains (as proposed in van der Schaft (2013)) in order to preserve a general approach. The PHS defined in (4) writes

$$\begin{cases}\partial_t\boldsymbol{X} &= (\boldsymbol{J} - \boldsymbol{R})\nabla H + \boldsymbol{G}\boldsymbol{u} + \boldsymbol{B}\boldsymbol{\lambda},\\ \boldsymbol{y} &= \boldsymbol{G}^T\nabla H,\\ \mathbf{0}_{C\times 1} &= \boldsymbol{B}^T\nabla H,\end{cases}$$

where the third line defines the algebraic constraints and the term $\boldsymbol{B}\boldsymbol{\lambda}$ the reaction to these constraints in the dynamics.

These constraints can be resolved leading to a reduced-order PHS using the change of variable $\boldsymbol{Z} = \mathcal{P}\boldsymbol{X}$, and splitting vector $\boldsymbol{Z}$ into two parts $\boldsymbol{Z}_1$ and $\boldsymbol{Z}_2$. This provides the system to be solved, more details can be found in Cardoso Ribeiro (2016).

3. SIMULATION: PASSIVE-GUARANTEED NUMERICAL METHODS

3.1 Discrete gradient

One major advantage of the PHS formalism is the ability to preserve the passivity (encoded in the infinite dimensional formulation) in the discrete time version required for simulation.

The discrete gradient (see Itoh and Abe (1988), Quispel and Turner (1996), and Gonzalez (2000)) is one way to preserve the passivity during simulation in discrete time steps. This approach is based on the chain rule to express the time derivative of the energy $E(t) = H \circ \boldsymbol{X}(t)$:

$$\frac{\mathrm{d}E(t)}{\mathrm{d}t} = \nabla H(\boldsymbol{X})\frac{\mathrm{d}\boldsymbol{X}(t)}{\mathrm{d}t}.$$

In the discrete time domain the variation of energy over time writes

$$\frac{\delta E(t,\delta t)}{\delta t} = \nabla_d H(\boldsymbol{X},\delta\boldsymbol{X})\frac{\delta\boldsymbol{X}(t,\delta t)}{\delta t},$$

with $\frac{\delta\boldsymbol{X}(t,\delta t)}{\delta t} = \frac{\boldsymbol{X}(t+\delta t)-\boldsymbol{X}(t)}{\delta t}$, and

$$[\nabla_d H(\boldsymbol{X},\delta\boldsymbol{X})]_i = \begin{cases}\dfrac{H_i(\boldsymbol{X}_i+\delta\boldsymbol{X}_i) - H_i(\boldsymbol{X}_i)}{\delta\boldsymbol{X}_i} & \text{if } \delta\boldsymbol{X}_i \neq 0,\\ \dfrac{\mathrm{d}H_i(\boldsymbol{X}_i)}{\mathrm{d}\boldsymbol{X}_i} & \text{else.}\end{cases} \tag{6}$$

In the case where the Hamiltonian is quadratic (i.e. $H(\boldsymbol{X}) = \frac{1}{2}\boldsymbol{X}^T\boldsymbol{Q}\boldsymbol{X}$) the discrete gradient defined in (6) gives (see (Aoues, 2014, Apdx 1)):

$$\nabla_d H(\boldsymbol{X},\delta\boldsymbol{X}) = \boldsymbol{Q}\left(\boldsymbol{X} + \frac{1}{2}\delta\boldsymbol{X}\right).$$

3.2 Explicit numerical scheme based on quadratization

Linearized system In the linear case ($\epsilon = 0$), the discrete version of the Hamiltonian (3) is quadratic, leading to the following numerical scheme

$$\begin{aligned}\frac{\delta\boldsymbol{X}(t,\delta t)}{\delta t} &= (\boldsymbol{J} - \boldsymbol{R})\nabla_d H(\boldsymbol{X},\delta\boldsymbol{X}) + G\boldsymbol{u},\\ \delta\boldsymbol{X}(t,\delta t) &= \delta t\boldsymbol{A}^{-1}\left((\boldsymbol{J} - \boldsymbol{R})\boldsymbol{Q}\boldsymbol{X} + \boldsymbol{G}\boldsymbol{u}\right)\end{aligned} \tag{7}$$

with $\boldsymbol{A} = \left(\boldsymbol{I} - \frac{\delta t}{2}(\boldsymbol{J} - \boldsymbol{R})\boldsymbol{Q}\right)$. This scheme is explicit and in this linear case, the discrete gradient is equivalent to the midpoint method (see (Aoues, 2014, Chap.2, §2.5)).

Quadratization method This method relies on two changes of variables in order to define a quadratic Hamiltonian. The first is the Cholesky decomposition and the second will consist in a quadratization of the resulting Hamiltonian as proposed in Lopes et al. (2015) for PHS (see Hélie (2022) for more details). Such an approach can be found for nonlinear string simulation in Ducceschi and Bilbao (2022) and Bilbao et al. (2023) using a different quadratization based on an auxiliary variable.

3.2.2.1. Cholesky decomposition In order to turn the non-separable quadratic part of the Hamiltonian into a separable one (in other words replacing $\boldsymbol{Q}$ by the identity matrix), the Cholesky decomposition will provide a first change of variables. Writing $\boldsymbol{Q} = \begin{bmatrix}T_0\boldsymbol{K} & \mathbf{0}_N\\ \mathbf{0}_N & \boldsymbol{M}^{-1}\end{bmatrix}$ as the product $\boldsymbol{L}^T\boldsymbol{L}$, new variables $\bar{\boldsymbol{W}} = \boldsymbol{L}_Q\boldsymbol{W}$ and $\bar{\boldsymbol{P}} = \boldsymbol{L}_P\boldsymbol{P}$ are defined (where $\boldsymbol{L} = \begin{pmatrix}\boldsymbol{L}_Q & \mathbf{0}_N\\ \mathbf{0}_N & \boldsymbol{L}_P\end{pmatrix}$). The Hamiltonian associated with the new PHS

$$\begin{pmatrix}\partial_t\bar{\boldsymbol{W}}(t)\\ \partial_t\bar{\boldsymbol{P}}(t)\end{pmatrix} = \boldsymbol{L}\begin{pmatrix}\mathbf{0}_N & \boldsymbol{I}_N\\ -\boldsymbol{I}_N & -\mathbf{C}\end{pmatrix}\boldsymbol{L}^T\begin{pmatrix}\bar{T}(t)\bar{\boldsymbol{W}}\\ \bar{\boldsymbol{P}}\end{pmatrix} + \begin{pmatrix}\mathbf{0}_N\\ \boldsymbol{I}_N\end{pmatrix}\boldsymbol{F}(t),$$
$$\bar{\boldsymbol{X}} = \left(\bar{\boldsymbol{J}} - \bar{\boldsymbol{R}}\right)\nabla\bar{H} + \bar{\boldsymbol{G}}\boldsymbol{F}.$$

becomes

$$\bar{H}(\bar{\boldsymbol{X}}) = \frac{1}{2}\left(\bar{\boldsymbol{P}}^T\bar{\boldsymbol{P}} + \bar{\boldsymbol{W}}^T\bar{\boldsymbol{W}}\right) + \alpha\left(\bar{\boldsymbol{W}}^T\bar{\boldsymbol{W}}\right)^2,$$

with $\bar{T}(t) = \left(1 + 2\alpha\bar{\boldsymbol{W}}^T\bar{\boldsymbol{W}}\right)$ and $\alpha = \frac{\epsilon}{4T_0}$.

3.2.2.2. Quadratization method The new state variables are defined by

$$\hat{\boldsymbol{X}}_i = sign(\bar{\boldsymbol{X}}_i)\big(2H(0,\dots,0,\bar{\boldsymbol{X}}_i,\bar{\boldsymbol{X}}_{i+1},\dots,\bar{\boldsymbol{X}}_N) - 2H(0,\dots,0,\bar{\boldsymbol{X}}_{i+1},\bar{\boldsymbol{X}}_{i+2},\dots,\bar{\boldsymbol{X}}_N)\big)^{1/2}, \quad (8)$$

leading to

$$\hat{\boldsymbol{W}}_i = sign(\bar{\boldsymbol{W}}_i)\sqrt{2\alpha\bar{\boldsymbol{W}}_i^4 + \left(1+4\alpha\left(\bar{\boldsymbol{W}}_{i+1}^2 + ... + \bar{\boldsymbol{W}}_N^2\right)\right)\bar{\boldsymbol{W}}_i^2}$$

and $\hat{\boldsymbol{P}}_i = sign(\bar{\boldsymbol{P}}_i)\sqrt{\bar{\boldsymbol{P}}_i^2}$.

Defining $\partial_t\hat{\boldsymbol{X}} = \mathfrak{J}(\hat{\boldsymbol{X}})\partial_t\bar{\boldsymbol{X}}$, where $\mathfrak{J}$ is the Jacobian of the change of variable (more details can be found in appendix A), the new PHS writes

$$\begin{pmatrix}\partial_t\hat{\boldsymbol{W}}(t)\\ \partial_t\hat{\boldsymbol{P}}(t)\end{pmatrix} = \mathfrak{J}(\hat{\boldsymbol{X}})\left(\bar{\boldsymbol{J}}-\bar{\boldsymbol{R}}\right)\mathfrak{J}^T(\hat{\boldsymbol{X}})\begin{pmatrix}\hat{\boldsymbol{W}}\\ \hat{\boldsymbol{P}}\end{pmatrix} + \mathfrak{J}(\hat{\boldsymbol{X}})\bar{\boldsymbol{G}}\boldsymbol{F}(t),$$

with the following Hamiltonian

$$\hat{H}(\hat{\boldsymbol{X}}) = \frac{1}{2}\left(\hat{\boldsymbol{P}}^T\hat{\boldsymbol{P}} + \hat{\boldsymbol{W}}^T\hat{\boldsymbol{W}}\right).$$

Using the time approximation $\partial_t\hat{\boldsymbol{X}} \approx \frac{\delta\hat{\boldsymbol{X}}}{\delta t}$ and the space approximation $\nabla_{\hat{\boldsymbol{X}}}\hat{H} \approx \nabla_d\hat{H} = \hat{\boldsymbol{X}} + \frac{\delta\hat{\boldsymbol{X}}}{2}$, the explicit numerical scheme (7) can be used for the variable $\hat{\boldsymbol{X}}$. Finally the result is given by recovering the initial variables $\delta\boldsymbol{X} = \boldsymbol{L}^{-1}\mathfrak{J}^{-1}(\hat{\boldsymbol{X}})\delta\hat{\boldsymbol{X}}$.

4. NUMERICAL RESULTS

Numerical simulations are performed for a string with homogeneous Dirichlet boundary conditions. The string is submitted to an excitation force $f(\xi,t) = f_{max}\frac{\cos(\pi(\xi-\xi_0))}{\ell}\frac{t}{T}$ for $0 < t \leq T = 0.01$ s and for $\xi_0 - \frac{\ell}{2} < \xi < \xi_0 + \frac{\ell}{2}$ with $\ell = 0.04$ m. The sampling frequency is $f_s = \frac{1}{t_s} = 44100$ Hz.

Table 1. Physical parameters used for the simulation of the string model (1)

Length	$L = 1.8$ m
Cross-section area	$A = \pi r^2 \approx 7.1\times10^{-6}$ m^2
Linear mass	$\mu = \rho A = 0.0551$ kg·m^{-1}
Viscous damping	$\alpha = 0.3$ s^{-1}
First eigenfrequency	$f_0 = 55$ Hz
Tension	$T_0 = 4L^2 f_0^2\mu \approx 2162$ N
Young's modulus	$E = 2\times10^{11}$ Pa

4.1 Eigenfrequencies and pitch gliding

Simulation have been performed with $f_{max} = 1500$ N·m^{-1} which is a value large enough to hear nonlinear phenomena. In this case, the "pitch glide" that can be seen in Fig. 1 is an increase of the harmonic's frequencies due to the stiffening effect present in the Hamiltonian. When there is damping, the loss of energy reduces the amplitude of vibration and therefore the values of those frequencies which tend towards the linear system eigenfrequencies (here 55 Hz and its multiples).

4.2 Energy balance

The energy balance of the simulation can be checked using Figs. 2 and 3. Fig. 2a present the three components of the power balance in the discrete time domain (the energy variation, the instantaneous dissipated power and the power exchanged with the outside of system). The

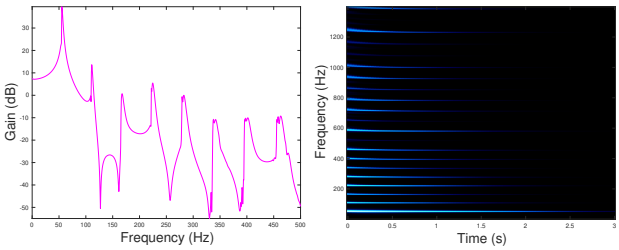

Fig. 1. Spectrum and spectrogram of the velocity signal at observation point $x_{obs} = 0.57L$.

fourth plot labeled "Sum" is the sum of these three power components, and should theoretically be equal to zero to verify the power balance. This sum is also displayed on its own in Fig. 2b as "Power Balance". The same plots in Fig. 3 are zoomed in on the time scale, to focus on the early stage of the simulation, and to clearly show the applied external force ($t \leq 0.01$ s) and the energy exchanges.

For $t > 0.01$ s, the system is no longer driven and oscillates freely, no power is exchanged with the outside, and the energy variation is due only to power dissipation.

The numerical error in the power balance of the system, shown in Fig. 3b, is quite low in comparison with the amplitude of the powers involved, however it is far from machine accuracy and it is unclear whether it can be solely attributed to floating-point error propagation. Additional error may be caused by the discretization of the external forces, the choice of the FEM method (instead of mixed finite elements) or the quadratization, which should be further investigated.

Disregarding the discretization of external forces and damping, it can be noticed in Fig. 4a that the energy variation in the case of a simulation without damping, and for $t > 0.01$ s (after the external force has been applied) is much lower (around 10^{-10}), it is associated to a relative error on the energy close to the machine accuracy as it can be seen in Fig. 4b.

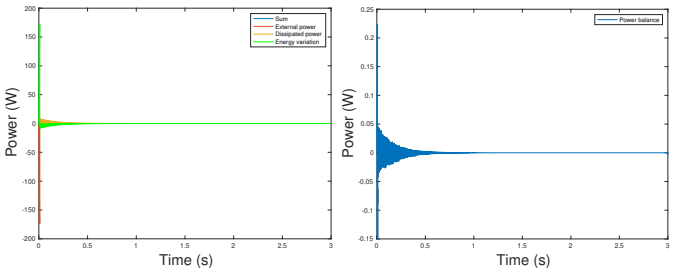

(a) Hamiltonian variation, dissipated and outgoing power (b) Power balance of the numerical simulation.

Fig. 2. Power balance of the numerical simulation.

4.3 Computation time

Regarding the computation time the use of quadratisation still involves more calculations than the linear problem. Indeed the matrix $\boldsymbol{A}$ varies with time (the Jacobian (A.1) has to be computed at each time step), therefore its inverse in (7) has to be computed at each time step. On a recent laptop using Matlab, the computation of 3 seconds of sound with 30 nodes requires approximately 30 seconds without any specific optimisation in the code.

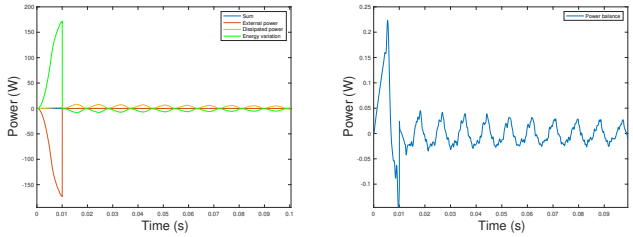

(a) Hamiltonian variation, dissipated and outgoing power (b) Power balance of the numerical simulation.

Fig. 3. Power balance of the numerical simulation (zoom on the beginning of the signal when the excitation force is applied ($t \leq 0.01$ s).

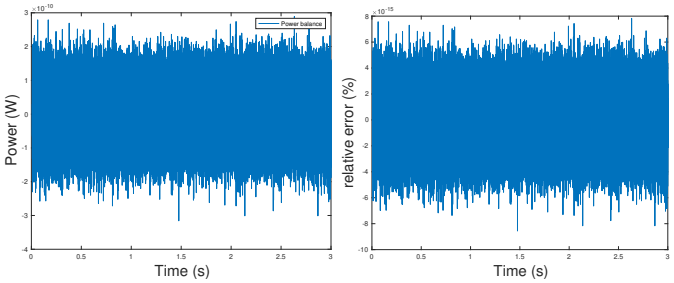

(a) Power balance of a numerical simulation without damping after input force has vanished ($t > 0.01$s). (b) Relative error in the energy variation $\frac{E(t_{n+1})-E(t_n)}{E(t_n)}$.

Fig. 4. Power balance and relative error on the energy of the numerical simulation without damping after input force has vanished ($t > 0.01$s).

5. CONCLUSION

This paper has introduced a Port-Hamiltonian formulation of a nonlinear string model discretized using the Finite Elements Method. This approach allows to use a power preserving numerical scheme in the time domain using a discrete gradient. Additionally, in the case of nonlinear systems using quadratization of the Hamiltonian turned the numerical scheme into an explicit one. The results of power balance are very satisfying for energy conservation in the case without damping and after an input force has been applied. In the general case, the power balance involves external and dissipated power and is not approximated with the same quality (power balance oscillations have an amplitude of 10^{-1} instead of 10^{-10}), this requires further work, which could be based on Mixed Elements Method (see Kotyczka et al. (2018)), or PFEM (see Cardoso-Ribeiro et al. (2020)) that have been already used when dealing with discretization and simulation of PHS.

In the context of sound synthesis the objectives of this work are to be able to simulate nonlinear system for different geometries (plates, shells, 3D structures) with a guaranteed power balance. Two major points have to be developed: (i) Extension to higher dimensional geometries has to be performed. Several results exist for plates (see e.g. Brugnoli et al. (2019a,b); Brugnoli and Matignon (2022)) using the discretization of the infinite dimensional Port-Hamiltonian system (Stokes-Dirac structure). This approach may be required to work with more general geometries. (ii) On the other hand, interactions between resonators (such as bowing, see e.g. Bilbao (2009); Chaigne and Kergomard (2016)), or striking, see Chabassier et al. (2013)) have to be defined in this PH formalism in order to connect resonators in a power preserving formalism with modularity (interconnection of PHS is a PHS).

ACKNOWLEDGEMENTS

The authors would like to thank, Thomas Hélie and Antoine Falaize for their fruitful discussion, and the reviewers for their comments which improved this paper.

REFERENCES

Anand, G.V. (1969). Large-amplitude damped free vibration of a stretched string. *The J. of the Acoust. Soc. of Am.*, 45(5), 1089–1096.

Aoues, S. (2014). *Schémas d'intégration dédiés à l'étude, l'analyse et la synthèse dans le formalisme Hamiltonien à ports*. Ph.D. thesis, INSA de Lyon.

Bilbao, S. (2009). *Numerical Sound Synthesis*. Wiley-Blackwell.

Bilbao, S., Ducceschi, M., and Zama, F. (2023). Explicit exactly energy-conserving methods for hamiltonian systems. *J. of Comput. Phys.*, 472, 111697.

Boffi, D., Brezzi, F., and Fortin, M. (2013). *Mixed Finite Element Methods and Applications*. Springer Berlin Heidelberg.

Brugnoli, A., Alazard, D., Pommier-Budinger, V., and Matignon, D. (2019a). Port-hamiltonian formulation and symplectic discretization of plate models part I: Mindlin model for thick plates. *Appl. Math. Model.*, 75, 940–960.

Brugnoli, A., Alazard, D., Pommier-Budinger, V., and Matignon, D. (2019b). Port-hamiltonian formulation and symplectic discretization of plate models part II: Kirchhoff model for thin plates. *Appl. Math. Model.*, 75, 961–981.

Brugnoli, A. and Matignon, D. (2022). A port-hamiltonian formulation for the full von-kármán plate model. In *10th European Nonlinear Dynamics Conference*, 85–86. Lyon, France.

Cardoso Ribeiro, F. (2016). *Port-Hamiltonian modeling and control of a fluid-structure system*. Ph.D. thesis, ISAE Sup Aéro, Université de Toulouse.

Cardoso-Ribeiro, F.L., Matignon, D., and Lefèvre, L. (2020). A partitioned finite element method for power-preserving discretization of open systems of conservation laws. *IMA J. of Math. Control and Inf.*, 38(2), 493–533.

Carrier, G. (1945). On the nonlinear vibration problem of the elastic string. *Q. of Appl. Math.*, 157–165.

Chabassier, J. (2012). *Modélisation et simulation numérique d'un piano par modèles physiques*. Ph.D. thesis, Ecole Polytechnique.

Chabassier, J., Chaigne, A., and Joly, P. (2013). Modeling and simulation of a grand piano. *The J. of the Acoust. Soc. of Am.*, 134(1), 648–665.

Chabassier, J. and Joly, P. (2010). Energy preserving schemes for nonlinear hamiltonian systems of wave equations: Application to the vibrating piano string. *Comput. Methods in Appl. Mech. and Eng.*, 199(45), 2779–2795.

Chaigne, A. and Kergomard, J. (2016). *Acoustics of Musical Instruments*. Springer New York.

Ducceschi, M. and Bilbao, S. (2022). Simulation of the geometrically exact nonlinear string via energy quadratisation. *J. of Sound and Vib.*, 534, 117021.

Geoffroy, T. (2019). *Synthèse sonore par modèles physiques dans le cadre d'une architecture d'électronique embarquée*. Master's thesis, Sorbonne Université, Paris, France.

Golo, G., Talasila, V., van der Schaft, A., and Maschke, B. (2004). Hamiltonian discretization of boundary control systems. *Autom.*, 40(5), 757–771.

Gonzalez, O. (2000). Exact energy and momentum conserving algorithms for general models in nonlinear elasticity. *Comput. Methods in Appl. Mech. and Eng.*, 190(13-14), 1763–1783.

Hélie, T. (2022). Elementary tools on Port-Hamiltonian Systems with applications to audio/acoustics. Lecture.

Itoh, T. and Abe, K. (1988). Hamiltonian-conserving discrete canonical equations based on variational difference quotients. *J. of Comput. Phys.*, 76(1), 85–102.

Kirchhoff, G. (1877). *Vorlesungen über mathematische Physik: Mechanik*. B. G. Teubner, Leipzig, Germany.

Kotyczka, P., Maschke, B., and Lefèvre, L. (2018). Weak form of stokes–dirac structures and geometric discretization of port-hamiltonian systems. *J. of Comput. Phys.*, 361, 442–476.

Lopes, N., Hélie, T., and Falaize, A. (2015). Explicit second-order accurate method for the passive guaranteed simulation of port-hamiltonian systems. In *IFAC-LHMNC*, volume 48, 223–228. Elsevier BV.

Maschke, B., Van Der Schaft, A.J., and Breedveld, P.C. (1992). An intrinsic hamiltonian formulation of network dynamics: Non-standard poisson structures and gyrators. *J. of the Frankl. Inst.*, 329(5), 923–966.

Narasimha, R. (1968). Non-linear vibration of an elastic string. *J. of Sound and Vib.*, 8(1), 134–146.

Quispel, G. and Turner, G. (1996). Discrete gradient methods for solving odes numerically while preserving a first integral. *J. of Phys. A: Math. and Gen.*, 29(13).

Raibaud, M. (2018). *Modélisation et simulation de systèmes discrétisés par la méthode des éléments finis dans le formalisme des Systèmes Hamiltoniens à Ports : application à la synthèse sonore*. Master's thesis, Sorbonne Université, Paris, France.

Rashad, R., Califano, F., van der Schaft, A.J., and Stramigioli, S. (2020). Twenty years of distributed port-hamiltonian systems: a literature review. *IMA J. of Math. Control and Inf.*, 37(4), 1400–1422.

Thoma, T. and Kotyczka, P. (2022). Explicit port-hamiltonian fem models for geometrically nonlinear mechanical systems. doi:10.48550/ARXIV.2202.02097.

Valette, C. and Cuesta, C. (1993). *Mécanique de la corde vibrante*. Hermes Sciences Publicat.

van der Schaft, A.J. (2013). Port-hamiltonian differential-algebraic systems. In *Surveys in Differential-Algebraic Equations I*, 173–226. Springer Berlin Heidelberg.

van der Schaft, A.J. and Maschke, B. (2002). Hamiltonian formulation of distributed-parameter systems with boundary energy flow. *J. of Geom. and Phys.*, 42(1), 166–194.

Watzky, A. (1992). Non-linear three-dimensional large-amplitude damped free vibration of a stiff elastic stretched string. *J. of Sound and Vib.*, 153(1), 125–142.

Wijnand, M., Hélie, T., and Roze, D. (2022). Finite-time tracking control of a nonlinear string to reference dynamics. In *ENOC 2020+2 (10th European Nonlinear Dynamics Conference)*, ENOC 2022 - Book of abstracts. Lyon, France.

Appendix A. QUADRATIZATION METHOD FOR THE NONLINEAR STRING MODEL

The Jacobian of the change of variable (8) is given by

$$\mathfrak{J} = \begin{pmatrix} \mathfrak{J}_Q & \mathbf{0}_N \\ \mathbf{0}_N & \mathfrak{J}_P \end{pmatrix}, \tag{A.1}$$

with the components of $\mathfrak{J}_Q$ defined by

$$\mathfrak{J}_{ii} = \frac{4\alpha\bar{\boldsymbol{W}}_i^3 + \left(1 + 4\alpha\left(\bar{\boldsymbol{W}}_{i+1}^2 + ... + \bar{\boldsymbol{W}}_N^2\right)\right)\bar{\boldsymbol{W}}_i}{\hat{\boldsymbol{W}}_i}$$

$$\mathfrak{J}_{ij_{(j>i)}} = \frac{4\alpha\bar{\boldsymbol{W}}_i^2\bar{\boldsymbol{W}}_j}{\hat{\boldsymbol{W}}_i} \quad \mathfrak{J}_{ij_{(j<i)}} = 0$$

$$\mathfrak{J}_{iN} = \frac{4\alpha\bar{\boldsymbol{W}}_i^2\bar{\boldsymbol{W}}_N}{\hat{\boldsymbol{W}}_i} \quad \mathfrak{J}_{NN} = \frac{4\alpha\bar{\boldsymbol{W}}_N^3 + \bar{\boldsymbol{W}}_N}{\hat{\boldsymbol{W}}_N}$$

and $\mathfrak{J}_P = \boldsymbol{I}_N$.

In order to write the new PHS, this Jacobian must be expressed as a function of $\hat{\boldsymbol{W}}_i$ which involves inverting the change of variable (8). This is done by solving the polynomial

$$2\alpha\bar{\boldsymbol{W}}_i^4 + \left(1 + 4\alpha\left(\bar{\boldsymbol{W}}_{i+1}^2 + ... + \bar{\boldsymbol{W}}_N^2\right)\right)\bar{\boldsymbol{W}}_i^2 - \hat{\boldsymbol{W}}_i^2 = 0,$$

which yields

$$\bar{\boldsymbol{W}}_i^2 = \frac{-\left(1 + 4\alpha\left(\bar{\boldsymbol{W}}_{i+1}^2 + \bar{\boldsymbol{W}}_{i+2}^2 + ... + \bar{\boldsymbol{W}}_N^2\right)\right) + \sqrt{\Delta_i}}{4\alpha},$$

where $\Delta_i = \left(1 + 4\alpha\left(\bar{\boldsymbol{W}}_{i+1}^2 + \bar{\boldsymbol{W}}_{i+2}^2 + ... + \bar{\boldsymbol{W}}_N^2\right)\right)^2 + 8\alpha\hat{\boldsymbol{W}}_i^2$.

Starting from $i = N-1$ it can be shown that $\Delta_i = \Delta_{i+1} + 8\alpha\hat{\boldsymbol{W}}_i^2$ with $\Delta_N = 1 + 8\alpha\hat{\boldsymbol{W}}_N^2$, and therefore

$$\bar{\boldsymbol{W}}_i^2 = \frac{-\sqrt{\Delta_{i+1}} + \sqrt{\Delta_i}}{4\alpha},$$

where Δ_i is a function of $\hat{\boldsymbol{W}}$ for all i.

Finally, the components of the Jacobian writes

$$\mathfrak{J}_{ii} = \frac{\sqrt{\Delta_i}}{\hat{\boldsymbol{W}}_i}\sqrt{\frac{\sqrt{\Delta_i} - \sqrt{\Delta_{i+1}}}{4\alpha}},$$

$$\mathfrak{J}_{ij_{j>i}} = \frac{\sqrt{\Delta_i} - \sqrt{\Delta_{i+1}}}{\hat{\boldsymbol{W}}_i}\sqrt{\frac{\sqrt{\Delta_j} - \sqrt{\Delta_{j+1}}}{4\alpha}},$$

$$\mathfrak{J}_{iN} = \frac{\sqrt{\Delta_i} - \sqrt{\Delta_{i+1}}}{\hat{\boldsymbol{W}}_i}\sqrt{\frac{\sqrt{\Delta_N} - 1}{4\alpha}},$$

$$\mathfrak{J}_{NN} = \frac{\sqrt{\Delta_N}}{\hat{\boldsymbol{W}}_N}\sqrt{\frac{\sqrt{\Delta_N} - 1}{4\alpha}}.$$